Journal of Materials Chemistry C

Accepted Manuscript

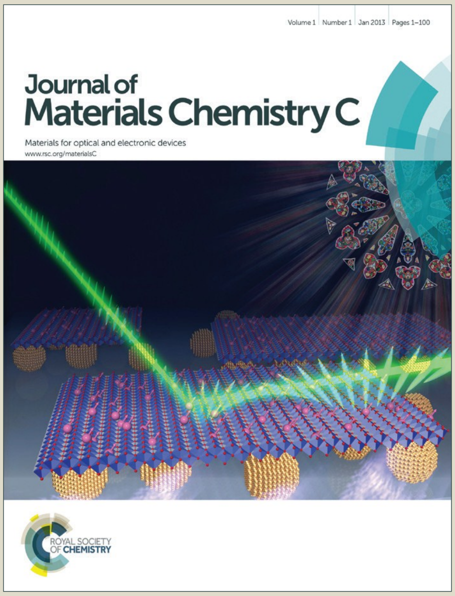

ROYAL SOCIETY OF CHEMISTRY

www.rsc.org/materialsC

Journal Name

ARTICLE

Received 00th January 20xx,
Accepted 00th January 20xx

DOI: 10.1039/x0xx00000x

www.rsc.org/

Thermally Tunable Circular Dichroism and Circularly Polarized Luminescence of Tetraphenylethene with Two Cholesterol Pendants

Qiang Ye[‡], Dandan Zhu[‡], Hongxing Zhang, Xuemin Lu, Qinghua Lu*

[‡] These authors contributed equally to this work.

This work provides a novel strategy for the construction of materials exhibiting circularly polarized luminescence (CPL) with thermally tunability and high efficiency in the solid state. In this strategy, cholesterol pendants were introduced into tetraphenylethene, a typical aggregation-induced emission (AIE) molecule using long undecyl spacers as covalent connection bridge. The resulting AIE molecule (**2CTPE**) exhibited CPL with a high dissymmetry factor (~10^{-2}) and high fluorescence efficiency (42%) in the solid state. The presence of the long spacer led the formation of a liquid crystal (LC) phase of **2CTPE** with typical focal conic texture of cholesteric LC, as revealed by polarizing obtical microscopy (POM) investigation. Furthermore, circular dichroism (CD) and CPL properties of **2CTPE** could be thermally regulated. These results give evidence to the synthesis of new, tunable CPL materials with high fluorescence efficiency in the solid state.

Introduction

Circularly polarized luminescence (CPL) is emission from a luminophore or an ensemble of luminophores with chirality. A CPL spectrum can reveal information on the stereochemistry, conformation, and three-dimensional structure of chiral materials in their excited electronic states.[1-5] CPL has become a useful tool for characterizing and quantifying the chirality of chiral materials. With the use of a suitable quarter-wave plate, CPL also can be transformed into linearly polarized light with little loss.[6] Therefore, CPL has promising applications in biosensing probes,[7, 8] in light-emitting diodes,[9-11] in optical amplifiers,[12] in color-image projection,[13] in optical information storage,[14, 15] in stereoscopic display,[16, 17] liquid crystal laser,[18] and, especially, in backlighting LCDs.[19-22]

In the past decades, organic conjugated compounds have attracted increasing interest in the construction of CPL materials because of their potentially advantageous electro-optical properties.[11] Recent studies have found that induction of chirality in achiral organic conjugated fluorogens via covalent linkages is an efficient strategy for generating materials exhibiting CPL.[15, 23-29] However, most of such materials suffer from aggregation-caused quenching due to the formation of species such as excimers and exciplexes in the condensed phase.[30, 31] Consequently, CPL barely manifests in the solid state, thus limiting the application of these materials.

Modulation of circularly polarized luminescence has a significant application in on-demand single-photon sources in photonics, optoelectronics, and quantum cryptography. Several systems with phototuning CPL property have been prepared. For example, Akagi reported reversible photoisomerization-enforced switching between emission and quenching of a CPL material based on poly(bithienylene-phenylene) with a quantum yield of 14–16% for the solid film.[32] However, preparation of a CPL material with tunable CPL property and high fluorescence efficiency in the condensed phase is still a challenge.

Liquid crystal (LC) molecules based on cholesterol possess a high degree of molecular chirality and can thus form periodic helical structures via molecular assembly. The cholesteric helical structure is a one-dimensional photonic crystal. Its band gap with spectral position is dependent on the helical pitch and is proportional to the average refractive index. As the helical pitch of this structure can be easily thermally controlled, selective and tunable light reflection can be achieved .[33, 34] Therefore, the modulation of the CPL of a compound with high fluorescence efficiency in the solid phase and cholesteric LC property also are of great interest.

In this work, a novel material, 4,4′ -bis[cholesteryl formate undecyloxy]tetraphenyl ethylene (**2CTPE**), was designed and synthesized. As a solid, **2CTPE** exhibited a high fluorescence quantum yield (42%) and excellent CPL performance. A focal conic texture of the cholesteric LC phase was observed.

Qiang Ye, Dandan Zhu, Hongxing Zhang, Prof. Xuemin Lu, Prof. Qinghua Lu
School of Chemistry and Chemical Engineering
Shanghai Jiao Tong University
800 Dongchuan Road, Shanghai 200240, China
E-mail: qhlu@sjtu.edu.cn

Electronic Supplementary Information (ESI) available: NMR spectra, HRMS spectrum, DSC curve, UV and FL spectra, UV transmission spectra, CD spectra. See DOI: 10.1039/x0xx00000x

Furthermore, the tunable CPL of the cholesteric LC system was realized by thermal control of the change in its helical pitch.

Results and Discussion

Synthesis and Characterization of 2CTPE

The synthetic routes for **2CTPE** are depicted in Scheme 1. According to a previous report, only a specific molecular modification of cholesterol can give rise to cholesteric LC property.[35] Thus, a long undecyl spacer was employed to ensure a suitable molecular flexibility of **2CTPE** and the formation of the cholesteric LC phase. The chemical structure of **2CTPE** were verified by NMR and HRMS measurements (shown in Figures S1–S3).

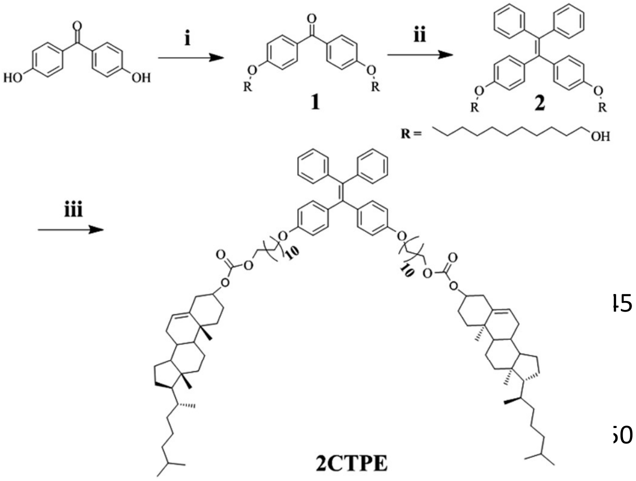

Scheme 1. Synthetic routes for **2CTPE:** Conditions: (i) 11-Bromo-1-undecanol, K_2CO_3, DMF, 90 °C, 24 h; (ii) benzophenone, $TiCl_4$, Zn, pyridine, THF, 70 °C, 48 h; (iii) cholesteryl chloroformate, pyridine, dimethylaminopyridine, THF, room temperature, 24 h.

Optical Properties

The optical properties of **2CTPE** were studied by UV/Vis spectroscopy and fluorescence spectroscopy. Figure 1a shows the UV/Vis absorption spectrum of a dichloromethane solution of **2CTPE** at a concentration of 5 × 10^{-5} M. The spectrum presents an obvious absorption peak at 332 nm corresponding to the π–π* transition of the tetraphenyl ethylene (TPE) moiety. Photoluminescence (PL) spectra of **2CTPE** in tetrahydrofuran (THF) and in THF/water mixtures were also recorded to check whether the modified TPE molecule still maintained aggregation-induced emission (AIE). As shown in Figure 1b, PL intensities of **2CTPE** at 375–390 nm decreased significantly with the increase in water fraction (f_w). However, the fluorescence emission shifted to 470 nm, and the intensity increased with increasing f_w value when the f_w value exceeded 80%. This phenomenon is attributed to AIE by **2CTPE** molecules. Because **2CTPE** is insoluble in water, the higher water content led to the aggregation of the molecules in the THF/water mixture. Fluorescence images of **2CTPE** in THF/water mixtures (inset of Figure 1b) suggest the same conclusion; f_w values of the mixtures irradiated at 365 nm by a UV lamp were 0%, 50%, 80%, and 95%. Because fluorescence emissions of **2CTPE** in THF/water mixtures with f_w values below 80% occurred at 375–390 nm, no light is observable in the fluorescence images. In contrast, **2CTPE** solutions with f_w values above 80% produced more green light, which is consistent with the emission peaks at 470 nm in the fluorescence spectra. These results prove that **2CTPE** showed typical AIE behavior due to the TPE moiety. In addition, the solution of 2CTPE in THF showed a quantum yield of 14% using quinine sulfate solution as standard. The steady-state and time-resolved fluorescence spectrofluorometry revealed that solid **2CTPE** exhibited a high quantum yield of 42%.

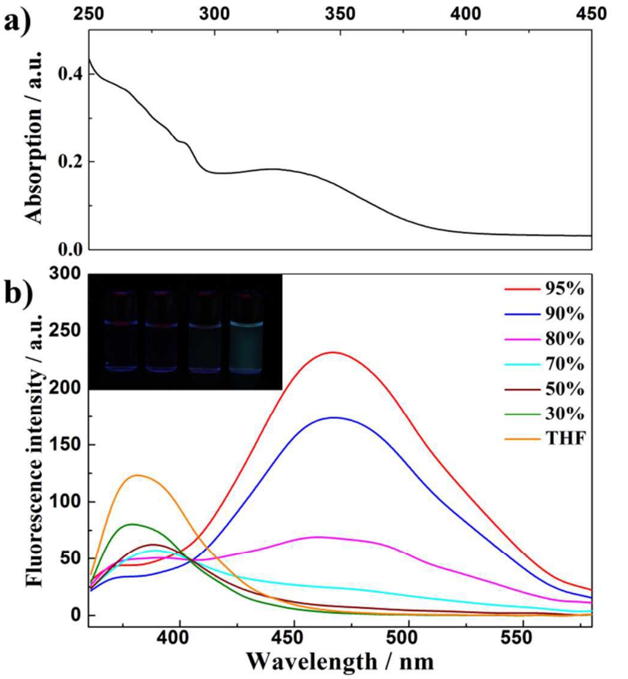

Figure 1. a) UV spectrum of **a** dichloromethane solution of **2CTPE** at a concentration of 5 × 10^{-5} M. b) Luminescence spectra of **2CTPE** in THF and THF/water mixtures with water fractions of 30%, 50%, 70%, 80%, 90%, and 95%. Excitation wavelength: 320 nm. Inset: fluorescence images of **2CTPE** in THF/water mixtures with water fractions of 0%, 50%, 80%, and 95% (from left to right). Photoluminescence experiments: 320 nm was used as excitation wavelength.

Liquid Crystalline Features

Cholesterol may form cholesteric LC phase upon a specific molecular modification. Thus, a long undecyl moiety was introduced into the target compound. The undecyl functioned as a spacer between TPE and cholesterol.

The differential scanning calorimetry (DSC) heating curve (see Figure S4) of **2CTPE** has endothermic peaks at 24 and 86 °C. As these peaks correspond to the melting point and clearing point (temperature of isotropic state, T_i), respectively, they indicate that **2CTPE** had a LC phase within a relatively wide temperature range (24–86 °C).

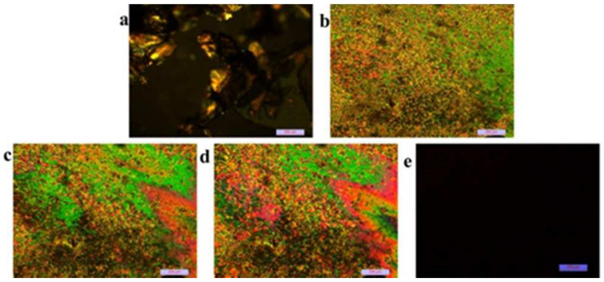

Figure 2. POM images of **2CTPE** at various temperatures: a) 20, b) 50, c) 60, d) 75, and e) 95 °C. Scale bar: 200 µm.

POM was employed to further observe the **2CTPE** phases at various temperatures. Figure 2a shows that amorphous and crystalline states coexisted in solid **2CTPE** at 20 °C. When the temperature was increased to 50 °C, a typical focal conic texture of the cholesteric LC phase could be observed, as shown in Figure 2b. This texture implies that **2CTPE** exhibited a cholesteric LC phase. With the continuous increase in temperature, no drastic changes in the texture structure occurred. However, the colors of the texture changed markedly. Compared with that in the POM image taken at 50 °C, the cholesteric LC texture became redder at 60 °C (Figure 2c). When the temperature increased to 75 °C, markedly redder textures appeared (Figure 2d). These results indicate that the cholesteric LC phase of **2CTPE** selectively reflected incident light, with the wavelength of reflected light varying with the temperature. The selectively reflected light tended to redshift with increasing temperature. This phenomenon be attributed to the increase in helical pitch of the **2CTPE** LC phase with the temperature increase. The temperature dependence of the helical pitch was also found in other cholesteric LC systems.[36, 37] When the temperature reached 95 °C, which exceeded T_i, the visual field became completely dark, and the LC phase completely disappeared (Figure 2f), implying that **2CTPE** molecules reached the isotropic state. This result demonstrates that **2CTPE** possesses thermotropic cholesteric LC phase and that the helical pitch is temperature-dependent.

Circular Dichroism (CD)

The CD spectrum can provide structural information about the ground electronic state of a chiral system. The CD value ($\Delta\varepsilon$) is the difference between the absorption of left- and right-circularly polarized light, $\Delta\varepsilon = \varepsilon_L - \varepsilon_R$, where ε_L and ε_R are, respectively, the left- and right-handed molar extinction coefficients for circularly polarized light. In general, The absorption dissymmetry factor (g_{abs}) is defined as: $g_{abs} = \Delta\varepsilon/\varepsilon = (\varepsilon_L - \varepsilon_R)/\varepsilon = 2(\varepsilon_L - \varepsilon_R)/(\varepsilon_L + \varepsilon_R)$, where ε_L and ε_R are the left- and right-handed molar extinction coefficients, respectively. To investigate the helical conformation and molecular arrangement of **2CTPE** in the LC state, CD spectra of **2CTPE** cast film were obtained at various temperatures. The cast film sample was treated at different temperature for 30 min, followed by cooling down to r.t., and then the CD investigation was performed at room temperature. The detection area is changed by varying the rotation angle of the film sample (See Figure S8-11).

As shown in Figure 3, the cast film showed positive bisignate Cotton effects (CEs) at room tempereature, negative CEs at 245 nm and positive CEs at 320 nm, corresponding to absorption bands of cholesteryl and TPE moieties, respectively. This result implies the successful transfer of chirality from cholesteryl to TPE moieties. In addition, the ε_L value was larger than ε_R because $\Delta\varepsilon = \varepsilon_L - \varepsilon_R > 0$. According to the exciton coupling theory, positive and negative CEs in CD spectra indicate right-handed (P-helicity) and left-handed (M-helicity) screw structures, respectively. Therefore, **2CTPE** in the cast film had *P*-helicity with a right-handed (clockwise) π-stacked structure. Notably, UV/Vis spectra of the cast film at different temperatures presented only tiny difference. However, intensities of both positive and negative CEs decreased with increasing temperature. At 50 °C, the CD signal of the cast film at the absorption band of the TPE moieties was much lower than the CD signal at the absorption band of the cholesteryl moiety. When the temperature reached 60 °C, there were almost no CD signals. The g_{abs} spectra of 2CTPE cast film treated at different temperature were shown in Figure 3 (lower). It is clear that the g_{abs} value decreased with the increasing temperatures. At room temperature, the film presented highest g_{abs} value at the absorption band of TPE moieties, which is 3.11×10^{-2} (345 nm). The CD results of varying rotation angle at different temperatures are shown in Figure S8, indicating that the anisotropy of the film is uniform.

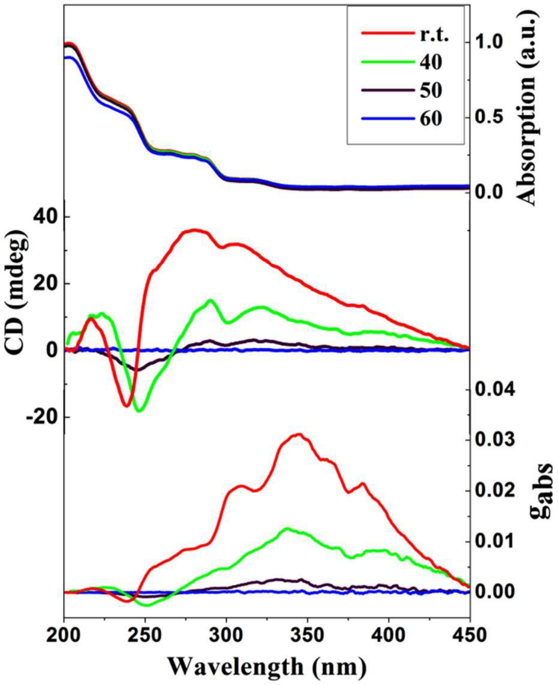

Figure 3. UV/Vis spectra (uppper), circular dichroism spectra (middle) and the absorption dissymmetry factor (g_{abs}) spectra (lower) of 2CTPE cast film located in the measurement chamber at different temperatures.

The difference in CD spectra at various temperatures proves the thermally tunable CD characteristic of **2CTPE**. According to the photonic band gap theory, the photonic band gap position of the cholesteric helical structure is determined by the helical pitch value. The change in helical pitch can shift the center position of the photonic band gap.[38-40] POM images obtained at various temperatures reveal that the helical pitch of the **2CTPE** LC phase increased with increasing temperature. The increase in helical pitch induced a shifting of the photonic band gap center to longer wavelength, thereby reducing the CD absorption intensity. Additionally, the shifting of the photonic band gap also was further confirmed by the UV transmission spectra of 2CTPE films (shown in Figure S7).

Circularly Polarized Luminescence

As the **2CTPE** film had intense fluorescence emission and strong CD signals, we anticipated that **2CTPE** had a CPL property in the excited state. CPL-active materials are generally evaluated by the luminescence dissymmetry factor (g_{lum}), which is defined by the expression $2(I_L - I_R)/(I_L + I_R)$. I_L and I_R correspond to the luminescence intensities of left-handed and right-handed polarized light, respectively. g_{lum} is an absolute value between 0 and 2, which denote linearly polarized, purely left-handed light or right-handed circular polarized light, respectively. In the present study, a Jasco CPL-200 was employed to investigate the CPL of **2CTPE** films; the g_{lum} value was directly obtained from the equipment.

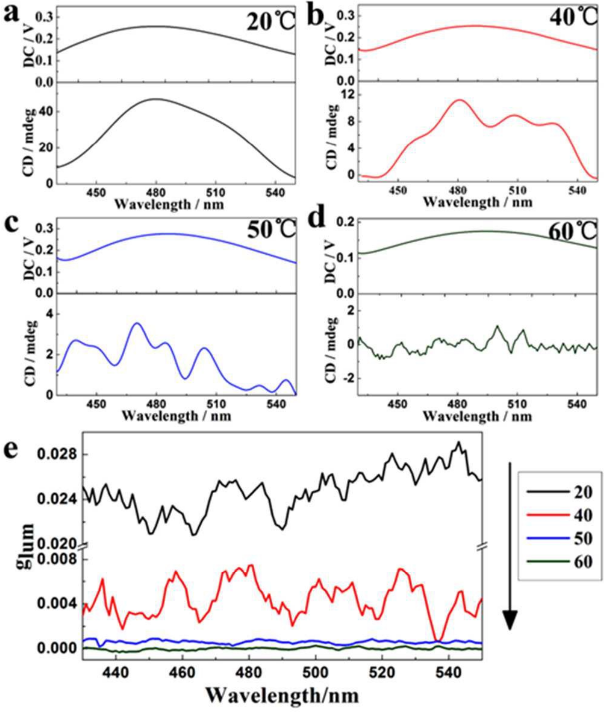

Figure 4. Circularly polarized luminescence spectra of **2CTPE** cast films treated at various temperatures: a) 20, b) 40, c) 50, and d) 60 °C (top: luminescence spectra, bottom: CPL spectra). e) Corresponding luminescence dissymmetry factors (g_{lum})

2CTPE films on quartz plates were subjected to various temperatures for 30 min and then measured on Jasco CPL-200 at room temperature. Upper curves in Figure 4a–4d are luminescence spectra for which DC was used to evaluate the PL intensity (I_{PL}). Lower curves are CPL spectra for which CD was used to evaluate the CPL intensity (I_{CPL}). Evidently, the **2CTPE** film had strong emission at a wavelength of 488 nm upon excitation by 360 nm wavelength, and the luminescence intensity hardly changed with temperature. All CPL spectra of **2CTPE** films showed positive CEs (lower curve in Figure 4a–4d), corresponding to left-handed CPL, which can be attributed to the *P*-helix structure (right-handed helicity) of the film. In addition, Figure 4a shows a high I_{CPL} value at 20 °C. When the temperature was below 50 °C, the film exhibited relatively intense CPL. However, when the temperature increased to 50 °C and above (Figure 4c, 4d), the I_{CPL} decreased markedly to a very low value. Figure 4e displays g_{lum} spectra of **2CTPE** film at various temperatures, and Table 1 summarizes the g_{lum} values. CPL spectra of the **2CTPE** film show high g_{lum} values at 20 °C (~10^{-2}). When the temperature increased to 40 °C, the g_{lum} values decreased to ~10^{-3}. When the temperature reached or exceeded 50 °C, g_{lum} values decreased to approximately 0. This CPL is consistent with the temperature-dependent change in CD.

Table 1. Summary of g_{lum} values of **2CTPE** cast films under various temperatures.

T (°C)	20	40	50	60
g_{lum} (λ, nm)[a]	2.54×10^{-2} (483)	7.45×10^{-3} (480)	7.52×10^{-4} (483)	~ 0

[a] Wavelength at which g_{lum} was evaluated.

To further clarify the assembled helical structure of solid-state **2CTPE**, the solvent dichloroethane in the **2CTPE**/TPE (molar ratio: 8/2) solution was removed by natural evaporation to induce the formation of assemblies. TPE was added to increase the helical pitch of the **2CTPE** assembly to a macroscopic level, in which the helical structure could be observed visually.[18] When the solvent was completely removed, a the macroscopic helical structure was obtained and was clearly observed with unaided vision, as shown by the photograph in Scheme 2. This structure was right-handed, in accordance with the CD and CPL results.

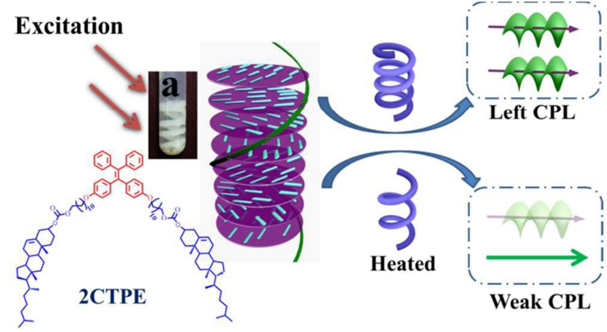

Scheme 2. A plausible model of the cholesteric liquid crystal structure and CPL emission of **2CTPE**. Inset: photograph of the macroscopic helical structure of **2CTPE**, which was obtained by natural evaporation of a 6 mL 20 mg/mL solution of **2CTPE/**TPE (8:2 molar ratio) in dichloroethane.

On the basis of the above investigation, we propose a plausible model of the cholesteric LC structure in Scheme 2. **2CTPE** forms a periodic helical structure via self-assembly during solvent evaporation because of molecular chirality. Formation is accompanied by a strong CD absorption and CPL with a g_{lum} value of 2.54×10^{-2}. With the temperature increase, the pitch of the helical structure increases, leading to a shift of the photonic band gap center to longer wavelength and reducing the CPL intensities. Moreover, our experiment proved that heat-treated **2CTPE** can restore all optical properties upon annealing in solution.

Conclusions

A novel CPL compound (**2CTPE**) with a high quantum yield (42%) in the solid state and a wide temperature range (24–86 °C) in the cholesteric LC phase was developed. The chiral center in the cholesteric moiety of **2CTPE** induces TPE moiety to generate circularly polarized luminescence was successfully achieved. Its CD and CPL could be finely tuned by changing the helical pitch of its LC phase by temperature changes. The **2CTPE** film had a high g_{lum} value, on the order of 10^{-2}. The chemical approach of combining AIE luminescence, chirality, and LC properties may enable access to thermally tunable high-performance CPL materials. Such materials may have applications in technologies such as chiral recognition and LC-based optoelectronic displays.

Experimental Section

Materials

Chemical reagents were purchased from J&K Scientific Co. and from Aldrich and were used as received. Solvents were purchased from the National Pharmaceutical Group Chemical Reagent Co. The solvent, THF, was dried over sodium and then distilled before use. Other solvents were used without purification.

Measurements

Nuclear magnetic resonance (NMR) spectra of samples in $CDCl_3$ were obtained on a Mercury Plus 400 spectrometer (Varian, Inc., USA). Tetramethylsilane was used (δ = 0) as internal reference. High-resolution mass spectrometry (HRMS) was performed on a SolariX-70FT-MS Fourier transform ion cyclotron resonance mass spectrometer (Bruker Daltonics, Germany) operated in MALDI mode. UV/Vis spectra and fluorescence spectra were obtained on a Lambda 20 UV/Vis spectrometer (Perkin Elmer, Inc., USA) and on an LS 50B spectrometer (Perkin Elmer, Inc., USA), respectively. The UV transmission study was carried out on a Lambda 750S UV/Vis spectrometer (Perkin Elmer, Inc., USA). Quantum yield of solid 2CTPE were measured on a QM/TM steady-state time-resolved fluorescence spectrofluorometer (PTI Company, USA). Fluorescence images of **2CTPE** solutions were taken when they were irradiated at 365 nm by using a commercially available UV lamp. DSC measurements were carried out on a Pyris 1 differential scanning calorimeter (Perkin Elmer, Inc., USA). Polarized optical images were captured under a Leica DM LP polarizing optical microscope (Leica Microsystems GmbH, Germany). The **2CTPE** cast film was prepared by dissolving **2CTPE** in dichloroethane to a concentration of 2 mg/mL and then casting the solution onto a quartz plate. In-situ CD measurements were performed after the temperature of the sample chamber was allowed to stabilize for 5 min. Non-in-situ CD study was carried out at room temperature after the heating treated film samples were cooling down. The detection area of CD is changed by varying the rotation angle of the film sample (0^o, 45^o, 90^o, 180^o, 270^o). CD spectra were recorded by using a Jasco J-815 CD spectrometer (Jasco, Japan), and CPL was measured on a Jasco CPL-200 spectrometer (Jasco, Japan).

Synthesis of Compound 1. 11-Bromo-1-undecanol (5.16 g, 20.6 mmol) was added to a mixture of 4,4'-dihydroxybenzophenone (2 g, 9.3 mmol), K_2CO_3 (7.75 g, 55.8 mmol), tetrabutylammonium bromide (30 mg), and 50 mL dimethylformamide under an argon atmosphere. The mixture was stirred at 90 °C for 24 h. After the mixture was cooled to room temperature, 200 mL of water was added, and the mixture was extracted thrice with 50 mL CH_2Cl_2. Portions of the organic layer were combined and washed with brine, dried over anhydrous magnesium sulfate, and evaporated to dryness under reduced pressure. The crude product was purified by column chromatography on silica gel using 1:2 (v/v) THF/ petroleum ether (PE) solution as eluent to yield **1** as a white solid (2.23 g, 43%). ^1H NMR (400 MHz, $CDCl_3$): δ 7.84–7.74 (m, 2H; Ar-*H*), 6.96 (dd, *J* = 8.7, 4.1 Hz, 2H; Ar-*H*), 4.13–4.00 (m, 2H; ArOC*H₂*), 3.70 (t, *J* = 6.6 Hz, 2H; HOC*H₂*), 1.85–1.76 (m, 2H; C*H₂*), 1.65–1.58 (m, 2H; C*H₂*), 1.45–1.29 (m, 14H; C*H₂*).

Synthesis of Compound 2. Under an argon atmosphere, a three-necked flask equipped with a magnetic stirrer was charged with zinc powder (9.8 g, 0.15 mol) and 280 mL of THF. The mixture was cooled in an ice–salt bath under vigorous stirring for 30 min, and then $TiCl_4$ (8.1 mL, 75 mmol) was slowly added by syringe. The suspension was warmed to room temperature, stirred for 0.5 h, and then heated with refluxing for 2.5 h. The mixture was again immersed in an ice–salt bath and cooled for 30 min, charged with pyridine (3 mL, 38 mmol), and then stirred for 20 min. A solution containing benzophenone (1.5 g, 8.2 mmol) and compound **1** (3.8 g, 6.8 mmol) in 80 mL THF was added slowly. The reaction mixture was then heated to reflux until the carbonyl compounds were consumed (reaction was monitored by thin-layer chromatography). An aqueous solution of 10% K_2CO_3 (100 mL) was added to quench the reaction, and then the mixture was thrice extracted with 100 mL of CH_2Cl_2. The organic layer was collected and concentrated. The crude product was purified by column chromatography on silica gel using ethyl acetate (1:4 (v/v) EA/PE solution) as eluent to yield compound **2** as a pale yellow solid (1.85 g, 31%). ^1H NMR (400 MHz, $CDCl_3$): δ 7.20–7.08 (m, 10H; Ar-*H*), 6.96–6.91 (m, 4H; Ar-*H*), 6.68–6.61 (m, 4H; Ar-*H*), 4.18–4.09 (m, 4H; ArOC*H₂*), 3.67 (t, *J* = 6.6 Hz, 4H; HOC*H₂*), 1.80–1.71 (m, 4H; C*H₂*), 1.63–1.54 (m, 4H; C*H₂*), 1.48–1.25 (m, 28H; C*H₂*).

Synthesis of 2CTPE. Compound **2** (705 mg, 1 mmol), pyridine (0.4 mL, 5 mmol), and dimethylaminopyridine (10 mg) were dissolved in 10 mL of THF, and the resulting mixture was then cooled in an ice bath under vigorous stirring for 30 min. Cholesterol chloroformate (0.98 g, 2.2 mmol) dissolved in 5 mL

THF was then added dropwise by using a constant-pressure dropping funnel. Afterward, the mixture was warmed to room temperature and stirred for 24 h. The solution was concentrated in a rotary evaporator and then extracted with CH_2Cl_2. The organic layer was separated and washed with brine, dried over anhydrous magnesium sulfate, evaporated to dryness under reduced pressure, and then purified by column chromatography on silica gel using 1:10 (v/v) EA/PE solution (0.7 g, 46%). ^{1}H NMR (400 MHz, $CDCl_3$): δ 7.16–7.02 (m, 5H; Ar-*H*), 6.97–6.93 (m, 2H; Ar-*H*), 6.66–6.63 (m, 2H; Ar-*H*;), 5.42 (d, *J* = 4.7 Hz, 1H; C=C*H*), 4.53–4.46 (m, 1H; OC*H*), 4.17–4.11 (m, 2H; ArOCH_2), 3.94–3.79 (m, 2H; COOCH_2), 2.45–2.40 (m, 2H; CH_2), 2.06–1.83 (m, 6H; CH_2), 1.78–1.59 (m, 8H; CH_2), 1.38–0.99 (m, 42H; C*H*,CH_2, CH_3), 0.70 (s, 3H; CH_3). ^{13}C NMR (101 MHz, $CDCl_3$): δ 157.62 (s), 154.69 (s), 144.38 (s), 139.42 (s), 132.87 (s), 131.38 (s), 127.64 (s), 125.97 (s), 122.90 (s), 113.47 (s), 77.63 (s), 67.84 (d, *J* = 11.7 Hz), 56.69 (s), 56.13 (s), 49.99 (s), 42.32 (s), 39.62 (d, *J* = 19.9 Hz), 38.07 (s), 36.87 (s), 36.55 (s), 36.19 (s), 35.80 (s), 31.88 (d, *J* = 6.9 Hz), 29.68–28.84 (m), 28.69 (s), 28.24 (s), 28.03 (s), 27.72 (s), 26.08 (s), 25.75 (s), 24.29 (s), 23.84 (s), 22.85 (s), 22.58 (s), 21.05 (s), 19.29 (s), 18.73 (s), 11.87 (s). HRMS (MALDI, *m*/*z*): $[M^+]$ calcd for $C_{104}H_{152}O_8$: 1530.31; found: 1530.15196.

Acknowledgements

This research was supported by the 973 Projects (2012CB933803, 2014CB643605), the National Science Fund for Distinguished Young Scholars (50925310), the National Science Foundation of China (21374060, 51173103), and the Excellent Academic Leaders of Shanghai (11XD1403000). The authors also thank Prof. Zhiyong Tang and Dr. Lin Shi (National Center for Nanoscience and Technology, China) for providing assistance with the CPL measurements.

Notes and references

1. I. Tinoco Jr, B. Ehrenberg and I. Z. Steinberg, *J. Chem. Phys.*, 1977, **66**, 916-920.
2. F. S. Richardson and J. P. Riehl, *Chem. Rev.* , 1977, **77**, 773-792.
3. J. P. Riehl, *Chem. Rev.*, 1986, **86**, 1-16.
4. A. S. Green, G. A. Gallup, M. A. Rosenberry and T. J. Gay, *Phys. Rev. Lett.*, 2004, **92**, 093201.
5. F. C. Spano, S. C. J. Meskers, E. Hennebicq and D. Beljonne, *J. Am. Chem. Soc.*, 2007, **129**, 7044-7054.
6. M. O'Neill and S. M. Kelly, *Adv. Mater.*, 2003, **15**, 1135-1146.
7. M. Iwamura, Y. Kimura, R. Miyamoto and K. Nozaki, *Inorg. Chem.* , 2012, **51**, 4094-4098.
8. G.-L. Law, C. M. Andolina, J. Xu, V. Luu, P. X. Rutkowski, G. Muller, D. K. Shuh, J. K. Gibson and K. N. Raymond, *J. Am. Chem. Soc.*, 2012, **134**, 15545-15549.
9. Emiel Peeters, Marwijn P. T. Christiaans, Rene´ A. J. Janssen, Herman F. M. Schoo, Harry P. J. M. Dekkers and E. W. Meijer, *J. Am. Chem. Soc.* , 1997, **119**, 9909-9910.
10. M. Oda, H.-G. Nothofer, G. Lieser, U. Scherf, S. C. J. Meskers and D. Neher, *Adv. Mater.* , 2000, **12**, 362-365.
11. Y. Gao, Y. Cui, J. K. Chan and C. J. Xu, *Am. J. Nucl. Med. Mol. Imaging*, 2013, **3**, 232-246.
12. H. P. J. M. Dekkers, P. F. Moraal, J. M. Timper and J. P. Riehl, *Appl. Spectrosc.*, 1985, **39**, 818-821.
13. S. H. Chen, D. Katsis, A. W. Schmid, J. C. Mastrangelo, T. Tsutsui and T. N. Blanton, *Nature*, 1999, **397**, 506-508.
14. X. Pan, S. F. Xiao, C. S. Wang, P. Cai, X. M. Lu and Q. H. Lu, *Opt. Commun.*, 2009, **282**, 763-768.
15. J. Z. Liu, H. M. Su, L. M. Meng, Y. H. Zhao, C. M. Deng, J. C. Y. Ng, P. Lu, M. Faisal, J. W. Y. Lam, X. H. Huang, H. K. Wu, K. S. Wong and B. Z. Tang, *Chem. Sci.*, 2012, **3**, 2737-2747.
16. D. R. Hall and P. A. Johnson, Google Patents, 1998.
17. P. Boher, T. Leroux, T. Bignon and V. Collomb-Patton, in *IS&T/SPIE Electronic Imaging*, International Society for Optics and Photonics, 2010, pp. 75240R-75240R-75212.
18. C. Mowatt, S. M. Morris, M. H. Song, T. D. Wilkinson, R. H. Friend and H. J. Coles, *J. Appl. Phys.*, 2010, **107**, 043101.
19. V. G. Chigrinov, *Electrooptic effects in liquid crystal materials*, Springer Science & Business Media, 1996.
20. Martin Grell and D. D. C. Bradley, *Adv. Mater.*, 1999, **11**, 895-905.
21. P. Fischer and F. Hache, *Chirality*, 2005, **17**, 421-437.
22. S. Relaix, C. Bourgerette and M. Mitov, *Appl. Phys. Lett.*, 2006, **89**, 251907.
23. K. Goto, R. Yamaguchi, S. Hiroto, H. Ueno, T. Kawai and H. Shinokubo, *Angew. Chem. Int. Ed.*, 2012, **51**, 10333-10336.
24. Y. Haketa, Y. Bando, K. Takaishi, M. Uchiyama, A. Muranaka, M. Naito, H. Shibaguchi, T. Kawai and H. Maeda, *Angew. Chem. Int. Ed.*, 2012, **51**, 7967-7971.
25. T. Kaseyama, S. Furumi, X. Zhang, K. Tanaka and M. Takeuchi, *Angew. Chem. Int. Ed.*, 2011, **50**, 3684-3687.
26. T. Ikeda, T. Masuda, T. Hirao, J. Yuasa, H. Tsumatori, T. Kawai and T. Haino, *Chem. Commun.*, 2012, **48**, 6025-6027.
27. T. Nehira, C. A. Parish, S. Jockusch, N. J. Turro, K. Nakanishi and N. Berova, *J. Am. Chem. Soc.*, 1999, **121**, 8681-8691.
28. J. Kumar, T. Nakashima, H. Tsumatori and T. Kawai, *J. Phys. Chem. Lett.*, 2014, **5**, 316-321.
29. H. K. Li, J. Cheng, Y. H. Zhao, J. W. Y. Lam, K. S. Wong, H. K. Wu, B. S. Li and B. Z. Tang, *Mater. Horiz.*, 2014, **1**, 518-521.
30. Y. Hong, J. W. Lam and B. Z. Tang, *Chem. Commun.*, 2009, 4332-4353.
31. J. W. Y. L. Yuning Hong, Ben Zhong Tang, *Chem. Soc. Rev.*, 2011, **40**, 5361–5388.
32. H. Hayasaka, T. Miyashita, K. Tamura and K. Akagi, *Adv. Funct. Mater.*, 2010, **20**, 1243-1250.
33. K. Bjorknas, P. Raynes and S. Gilmour, in *International Symposium on Optical Science and Technology*, International Society for Optics and Photonics, 2002, pp. 122-133.
34. S. H. Chen, D. Katsis, A. W. Schmid, J. C. Mastrangelo, T. Tsutsui and T. N. Blanton, *Nature*, 1999, **397**, 506-508.
35. K. Kawabata and H. Goto, *Chem. Eur. J.*, 2012, **18**, 15065-15072.
36. R. W. Guo, K. X. Li, H. Cao, X. J. Wu, G. J. Wang, Z. H. Cheng, F. F. Wang, H. Q. Zhang and H. Yang, *Polymer*, 2010, **51**, 5990-5996.
37. F. F. Wang, K. X. Li, P. Song, X. J. Wu, H. P. Chen and H. Cao, *Compos. Part B-Eng.*, 2013, **46**, 145-150.
38. R. R. Parsons, *Phys. Rev. Lett.*, 1969, **23**, 1152-1154.
39. A. Bobrovsky, V. Shibaev and J. Stumpe, *J. Phys. Chem. A* 2006, **110**, 2331-2336.
40. J. Xu, A. Lakhtakia, J. Liou, A. Chen and I. J. Hodgkinson, *Opt. Commun.*, 2006, **264**, 235-239.

Table of contents

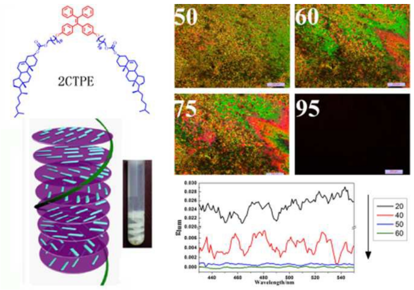

A novel l cholesteric liquid crystal molecule 2CTPE with thermally tunable CPL property based on cholesterol and tetraphenylethylene was successfully synthesized.